Contribution from the Department of Chemistry,
Michigan State University, East Lansing, Michigan 48824

Crystal Structures and Properties of Two Sodides and an Electride

Steven B. Dawes, Donald L. Ward, Odette Fussa-Rydel, Rui-H. Huang, and James L. Dye*

Received June 23, 1988

The crystal structures of $Rb^+(15\text{-crown-}5)_2Na^-$ (I) (monoclinic, space group $C2/m$, a = 11.555 (3) Å, b = 13.587 (3) Å, c = 9.958 (3) Å, β = 92.03 (2)°, V = 1562.4 (7) Å^3, Z = 2) and $Cs^+(18\text{-crown-}6)_2Na^-$ (II) (monoclinic, space group $C2/c$, a = 13.581 (3) Å, b = 15.684 (2) Å, c = 17.429 (4) Å, β = 93.16 (2)°, V = 3706.8 (15) Å^3, Z = 4) have been determined by single-crystal X-ray diffraction. The agreement factors are R = 0.044 and R_w = 0.052 for I and R = 0.028 and R_w = 0.033 for II. These structures show that the large complexed cations form closest packed arrays, leaving well-defined anionic sites that are isolated from each other, except for rather constricted channels that interconnect them. Each anionic site is surrounded by eight complexed cations and by six other anionic sites. The sodide $Cs^+(18C6)_2Na^-$ is isostructural with the electride $Cs^+(18C6)_2e^-$ [Dawes, S. B.; Ward, D. L.; Huang, R. H.; Dye, J. L. *J. Am. Chem. Soc.* **1986**, *108*, 3534], and indeed, Na^- can be substituted for e^- in one, two, or three sites around the complexed cesium cation as shown by ^{133}Cs MAS NMR studies [Dawes, S. B.; Ellaboudy, A. S.; Dye, J. L. *J. Am. Chem. Soc.* **1987**, *109*, 3508]. The implications of the structures of the alkalides and their similarity to the electride structure are discussed in relation to electron localization in the latter compound.

Introduction

Alkalides and electrides are two classes of crystalline ionic compounds that consist of complexed alkali-metal cations and either alkali metal anions or trapped electrons.[1-30] The "parent compound", Na^+(cryptand[2.2.2])Na^- was, until recently, the only alkalide of known crystal structure.[2] Recent improvements in synthesis techniques[17,20] have yielded new sodides, potassides, rubidides, cesides, and electrides and larger and better quality crystals.[26,29,31]

The general structural features of the electride $Cs^+(18\text{-crown-}6)_2e^-$ were reported previously.[26] The salt consists of cesium cations, each of which is complexed by two 18-crown-6 (18C6)[32] molecules that pack together in such a way that anionic sites of >4 Å diameter are produced. The structure supports the conjecture that this electride contains localized electrons whose charge distribution is centered at the anionic sites (cavities) and which do not interact strongly with each other or with the cations. The extent of overlap with the $-CH_2-$ groups that line the cavity is not known at this time.

The rubidium EXAFS studies[22,33] showed that the complexed rubidium cation in alkalides and electrides has normal Rb^+–O and Rb^+–C distances.[22,33] The large diamagnetic shifts of alkali-metal anions in crystalline alkalides permitted the positive identification of Na^-,[19,25] K^-,[23] Rb^-,[24] and Cs^-[15,16,30] by alkali-metal MAS-NMR spectroscopy. Static NMR studies of line widths and shapes showed that the NMR spectrum of Na^+(C222) is primarily influenced by both dipolar and quadrupolar effects,[25] that of Na^- by dipolar coupling to the $-CH_2-$ protons of the cryptand,[25] and that of complexed Cs^+ by dipolar coupling and chemical shift anisotropy.[30]

The chemical shift of complexed Cs^+ in the pure sodide, −61 ppm, is characteristic of $Cs^+(18C6)_2$ in diamagnetic alkalides and in model salts that contain this cation.[30] In the pure electride, the MAS-NMR peak position is paramagnetically shifted and changes with temperature in accord with the Curie law because of the presence of unpaired electrons, but the electron density at the cesium nucleus is only 0.033% that of the free atom.[30] Three

(1) Dye, J. L.; Ceraso, J. M.; Lok, M. T.; Barnett, B. L.; Tehan, F. J. *J. Am. Chem. Soc.* **1974**, *96*, 608.
(2) Tehan, F. J.; Barnett, B. L.; Dye, J. L. *J. Am. Chem. Soc.* **1974**, *96*, 7203.
(3) Dye, J. L.; Andrews, C. W.; Mathews, S. E. *J. Phys. Chem.* **1975**, *79*, 3065.
(4) Dye, J. L. *Sci. Am.* **1977**, *237*(July), 92.
(5) Dye, J. L. *J. Chem. Educ.* **1977**, *54*, 332.
(6) Dye, J. L.; Yemen, M. R.; DaGue, M. G.; Lehn, J.-M. *J. Chem. Phys.* **1978**, *68*, 1665.
(7) Dye, J. L. *Angew. Chem.* **1979**, *18*, 587.
(8) DaGue, M. G.; Landers, J. S.; Lewis, H. L.; Dye, J. L. *Chem. Phys. Lett.* **1979**, *66*, 169.
(9) Dye, J. L.; DaGue, M. G.; Yemen, M. R.; Landers, J. S.; Lewis, H. L. *J. Phys. Chem.* **1980**, *84*, 1096.
(10) Landers, J. S.; Dye, J. L.; Stacy, A.; Sienko, M. J. *J. Phys. Chem.* **1981**, *85*, 1096.
(11) Le, L. D.; Issa, D.; VanEck, B.; Dye, J. L. *J. Phys. Chem.* **1982**, *86*, 7.
(12) VanEck, B.; Le, L. D.; Issa, D.; Dye, J. L. *Inorg. Chem.* **1982**, *21*, 1966.
(13) Schindewolf, U.; Le, L. D.; Dye, J. L. *J. Phys. Chem.* **1982**, *86*, 2284.
(14) Issa, D.; Dye, J. L. *J. Am. Chem. Soc.* **1982**, *104*, 3781.
(15) Ellaboudy, A.; Dye, J. L.; Smith, P. B. *J. Am. Chem. Soc.* **1983**, *105*, 6490.
(16) Dye, J. L.; Ellaboudy, A. *Chem. Br.* **1984**, *20*, 210.
(17) Dye, J. L. *J. Phys. Chem.* **1984**, *88*, 3842.
(18) Issa, D.; Ellaboudy, A.; Janakiraman, R.; Dye, J. L. *J. Phys. Chem.* **1984**, *88*, 3847.
(19) Ellaboudy, A.; Tinkham, M. L.; VanEck, B.; Dye, J. L.; Smith, P. B. *J. Phys. Chem.* **1984**, *88*, 3852.
(20) Dye, J. L. *Prog. Inorg. Chem.* **1984**, *32*, 327.
(21) Jaenicke, S.; Dye, J. L. *J. Solid State Chem.* **1984**, *54*, 320.
(22) Fussa, O.; Kauzlarich, S.; Dye, J. L.; Teo, B. K. *J. Am. Chem. Soc.* **1985**, *107*, 3727.
(23) Tinkham, M. L.; Dye, J. L. *J. Am. Chem. Soc.* **1985**, *107*, 6129.
(24) Tinkham, M. L.; Ellaboudy, A.; Dye, J. L.; Smith, P. B. *J. Phys. Chem.* **1986**, *90*, 14.
(25) Ellaboudy, A.; Dye, J. L. *J. Magn. Reson.* **1986**, *66*, 491.
(26) Dawes, S. B.; Ward, D. L.; Huang, R. H.; Dye, J. L. *J. Am. Chem. Soc.* **1986**, *108*, 3534.
(27) Papaioannou, J.; Jaenicke, S.; Dye, J. L. *J. Solid State Chem.* **1987**, *67*, 122.
(28) Jaenicke, S.; Faber, M. K.; Dye, J. L.; Pratt, W. P. *J. Solid State Chem.* **1987**, *68*, 239.
(29) Dye, J. L.; DeBacker, M. G. *Annu. Rev. Phys. Chem.* **1987**, *38*, 271.
(30) Dawes, S. B.; Ellaboudy, A. S.; Dye, J. L. *J. Am. Chem. Soc.* **1987**, *109*, 3508.
(31) Huang, R. H.; Ward, D. L.; Kuchenmeister, M. E.; Dye, J. L. *J. Am. Chem. Soc.* **1987**, *109*, 5561.
(32) IUPAC names: 18-crown-6, 1,4,7,10,13,16-hexaoxacyclooctadecane, abbreviation 18C6; 15-crown-5, 1,4,7,10,13-pentaoxacyclopentadecane, abbreviation 15C5; cryptand[2.2.2], 4,7,13,16,21,24-hexaoxa-1,10-diazabicyclo[8.8.8]hexacosane, abbreviation C222.
(33) Fussa-Rydel, O.; Dye, J. L.; Teo, B. K. *J. Am. Chem. Soc.* **1988**, *110*, 2495.
(34) Gunn, S. R. *J. Chem. Phys.* **1967**, *47*, 1174.
(35) Copeland, D. A.; Kestner, N. R.; Jornter, J. *J. Chem. Phys.* **1970**, *53*, 1189.
(36) Kevan, L.; Bowman, M. K.; Nurayana, P. A.; Boeckman, R. K.; Yudanov, U. I.; Tsuetkov, Yu. D. *J. Chem. Phys.* **1975**, *63*, 409.
(37) Kevan, L. *J. Phys. Chem.* **1980**, *84*, 1232.
(38) Kevan, L. *Acc. Chem. Res.* **1981**, *14*, 138.
(39) Golden, S.; Tuttle, T. R., Jr. *J. Phys. Chem.* **1978**, *82*, 944.
(40) Golden, S.; Tuttle, T. R., Jr. *J. Chem. Soc., Faraday Trans. 2* **1979**, *75*, 474; **1981**, *77*, 889.
(41) Van Vleck, J. H. *Phys. Rev.* **1948**, *74*, 161.
(42) Cromer, D. J.; Waber, J. T. *International Tables for X-ray Crystallography*; Kynoch Press: Birmingham, England, 1974; Vol. IV, Table 2.2B.

0020-1669/89/1328-2132$01.50/0

Table I. Crystallographic Data for $Rb^+(15C5)_2Na^-$ (I) and $Cs^+(18C6)_2Na^-$ (II) at 213 K

	I	II
formula	$Rb^+(C_{10}H_{20}O_5)_2Na^-$	$Cs^+(C_{12}H_{24}O_6)_2Na^-$
fw	549.00	684.54
d_{calcd}, g/cm^3	1.17	1.23
a, Å	11.555 (3)	13.581 (3)
b, Å	13.587 (3)	15.684 (2)
c, Å	9.958 (3)	17.429 (4)
β, deg	92.03 (2)	93.16 (2)
V, Å^3	1562.4 (7)	3706.8 (15)
Z	2	4
space group	$C2/m$	$C2/c$
μ, cm^{-1}	15.9	10.5
transmissn coeff		0.83–1.0
R	0.044	0.028
R_w	0.052	0.033

additional lines of Cs^+ in the MAS-NMR spectrum of mixed electride–sodide samples[30] show that one, two, or three Na^- ions can substitute for e^- around a Cs^+ ion in $Cs^+(18C6)_2e^-$. Higher concentrations of Na^- result in phase separation.

Optical spectra,[15,16,20] magnetic susceptibilities,[18] ESR spectra,[18] and conductivities[15,16] support the model of electron trapping at all anionic sites in $Cs^+(18C6)_2e^-$, with such weak overlap of the wave functions of adjacent electrons that they behave nearly independently.

This paper describes the crystal structures of two sodides, $Rb^+(15C5)_2Na^-$ and $Cs^+(18C6)_2Na^-$. The similarity of the latter to the structure of $Cs^+(18C6)_2e^-$ provides important information about the nature of the electron-trapping site. The relation of the structures to the observed ^{133}Cs MAS-NMR spectra is also included.

Experimental Section

The synthesis of polycrystalline alkalides and electrides has been previously described in detail.[17,20] Since these materials react readily with air and moisture and decompose at temperatures above about 0 °C, special techniques were developed for crystal growth, selection, and mounting. In order to obtain high-quality crystals for X-ray diffraction studies, a polycrystalline sample was slowly recrystallized from an appropriate solvent mixture. A sealed glass tube that contained the cold polycrystalline sample was opened in a nitrogen-filled glovebag, and the sample was poured into the flat-bottomed, crystal-growing arm of a two-chamber H-cell. After evacuation to $\sim 10^{-5}$ Torr at −78 °C, enough dimethyl ether was distilled into the cell to form a nearly saturated deep blue solution (~5 mL). A less polar cosolvent (trimethylamine or diethyl ether) was then distilled into the cell to form a saturated soltuion that contained a small number of seed crystals at the desired recrystallization temperature. This temperature ranged from −15 °C for the more robust sodides to −40 °C for the electride. Crystals were grown by either slow distillation of the more volatile dimethyl ether to the other arm of the cell (maintained at a temperature of 5–10 °C below that of the crystal-growing chamber) or by slowly cooling the cell (typically 1 °C/h). Larger crystals could be grown by cycling processes; in the first case by repeatedly distilling some of the dimethyl ether back into the crystal-growing chamber and out again, and in the latter case by slowly ramping the temperature down and up several times over a 5 °C range, being careful not to exceed the saturation temperature. The solvent removal method has the advantage that the crystals are at a constant temperature. It is, however, far easier to grow crystals by the slow cooling method, since this process is easily automated.

After the crystals had been grown, the mother liquor was poured through a coarse frit into the other arm of the H-cell and the crystals were rinsed with diethyl ether or trimethylamine. The solvents were then removed by distillation and the cell was evacuated to $\sim 10^{-5}$ Torr while the crystals were kept cold. In most cases, the crystals were stored at −78 °C in a dry ice bath until needed.

For diffraction studies, the cold crystals were transferred in a nitrogen-filled glovebag to a shallow ramp-shaped well in a copper block maintained at −50 °C and covered with prepurified, cold *n*-octane. A suitable crystal was selected by examination with a long focal length microscope inserted through the glovebag. The crystal was moved up the ramp out of the octane and picked up on the tip of a glass or quartz fiber that had a small amount of hydrocarbon grease on its tip. The fiber had been previously mounted in a goniometer pin. The crystal was then moved to the diffractometer while in a constant flow of cold nitrogen and placed into the nitrogen-cooled goniometer. After a short period of time the octane sublimed from the crystal. Following this procedure, it was possible to collect data on these reactive, thermally unstable compounds without significant decomposition.

Table II. Positional Parameters and Their Estimated Standard Deviations for Non-Hydrogen Atoms in $Rb^+(15C5)_2Na^-$ at 213 K

atom	x	y	z	B,[a] Å^2
Rb1	0.500	0.000	0.500	3.89 (3)
Na1	0.500	0.500	0.000	7.7 (2)
O1	0.4537 (6)	0.000	0.1948 (7)	6.3 (2)
O4	0.5015 (4)	−0.1794 (4)	0.3268 (5)	6.1 (1)
O7	0.7204 (4)	−0.1047 (4)	0.4366 (6)	7.5 (2)
C2	0.3880 (7)	−0.0891 (6)	0.1675 (8)	6.4 (2)
C3	0.4714 (8)	−0.1713 (6)	0.1891 (8)	6.9 (2)
C5	0.6058 (8)	−0.2347 (6)	0.3525 (9)	8.0 (3)
C6	0.7115 (7)	−0.1780 (8)	0.335 (1)	9.1 (3)
C8a	0.823 (1)	−0.0331 (9)	0.465 (1)	5.6 (4)
C8b	0.811 (1)	0.053 (1)	0.370 (2)	7.1 (5)

[a] Values for anisotropically refined atoms are given in the form of the isotropic equivalent thermal parameter defined as $(4/3)[a^2B(1,1) + b^2B(2,2) + c^2B(3,3) + ab(\cos\gamma)B(1,2) + ac(\cos\beta)B(1,3) + bc(\cos\alpha)B(2,3)]$.

Table III. Positional Parameters and Their Estimated Standard Deviations for Non-Hydrogen Atoms in $Cs^+(18C6)_2Na^-$ at 213 K

atom	x	y	z	B,[a] Å^2
Cs1	0.000	0.02094 (3)	0.250	3.241 (7)
Na1	0.000	0.500	0.000	8.4 (1)
O1	−0.0980 (2)	0.1741 (2)	0.3653 (2)	4.42 (7)
O4	0.1135 (2)	0.1611 (2)	0.3643 (2)	4.49 (8)
O7	0.1361 (2)	−0.0171 (2)	0.4081 (2)	4.30 (7)
O10	−0.0224 (2)	−0.1364 (2)	0.3877 (2)	4.49 (7)
O13	−0.1820 (3)	−0.1166 (2)	0.2736 (2)	5.74 (9)
O16	−0.2335 (2)	0.0605 (2)	0.2861 (2)	5.24 (8)
C2	−0.0319 (4)	0.2435 (3)	0.3715 (3)	5.1 (1)
C3	0.0614 (4)	0.2169 (4)	0.4119 (3)	5.2 (1)
C5	0.1980 (4)	0.1252 (4)	0.4032 (3)	5.0 (1)
C6	0.1767 (4)	0.0506 (4)	0.4540 (3)	5.0 (1)
C8	0.1279 (4)	−0.0932 (4)	0.4518 (3)	5.1 (1)
C9	0.0766 (4)	−0.1601 (4)	0.4053 (3)	5.4 (1)
C11	−0.0822 (5)	−0.2029 (3)	0.3564 (3)	6.1 (1)
C12	−0.1830 (4)	−0.1706 (4)	0.3369 (3)	6.6 (1)
C14	−0.2755 (4)	−0.0767 (5)	0.2480 (4)	7.9 (2)
C15a	−0.307 (1)	0.003 (1)	0.274 (1)	10.6 (5)*
C15b	−0.3013 (7)	−0.0095 (6)	0.2990 (5)	4.0 (2)*
C17	−0.2617 (4)	0.1299 (4)	0.3319 (3)	5.8 (1)
C18	−0.1878 (4)	0.1982 (4)	0.3284 (3)	5.5 (1)

[a] Starred values indicate that atoms were refined isotropically. Values for anisotropically refined atoms are given in the form of the isotropic equivalent thermal parameter defined as $(4/3)[a^2B(1,1) + b^2B(2,2) + c^2B(3,3) + ab(\cos\gamma)B(1,2) + ac(\cos\beta)B(1,3) + bc(\cos\alpha)B(2,3)]$.

Table IV. Selected Values of Interatomic Distances (Å)[a]

	$Rb^+(15C5)_2Na^-$	$Cs^+(18C6)_2Na^-$	$Cs^+(18C6)_2e^-$
M^+–M^+	[4] 8.92	[2] 8.74	[2] 8.72
	[2] 9.96	[4] 10.38	[4] 10.27
N^-–N^-	[4] 8.92	[2] 8.71	[2] 8.68
	[2] 9.96	[4] 10.37	[4] 10.27
M^+–N^-	[2] 7.49	[2] 7.87	[2] 7.71
	[2] 7.75	[2] 8.28	[2] 8.00
M^+–O	[4] 8.42	[2] 8.69	[2] 8.67
		[2] 9.26	[2] 9.40
mean	3.02 (4)	3.36 (8)	3.35 (8)
max	3.067 (7)	3.468 (3)	3.457 (8)
min	2.986 (5)	3.287 (3)	3.296 (8)
C–C			
mean	1.49 (3)	1.47 (3)	1.49 (2)
max	1.51 (2)	1.505 (8)	1.52 (2)
min	1.459 (13)	1.41 (2)	1.47 (2)
C–O			
mean	1.45 (5)	1.42 (3)	1.42 (2)
max	1.554 (13)	1.463 (7)	1.44 (1)
min	1.408 (9)	1.35 (2)	1.39 (2)

[a] Numbers in brackets are multiplicities.

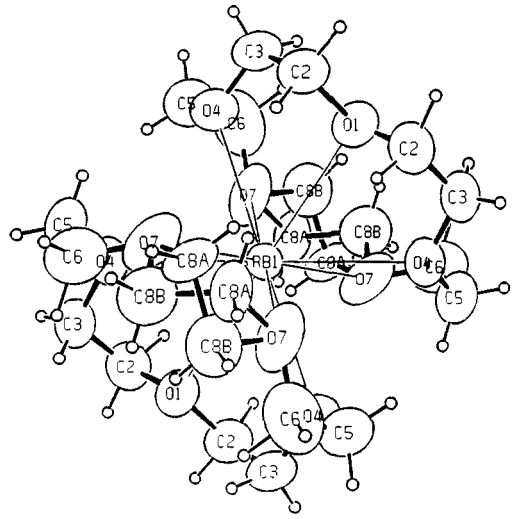

Figure 1. Single molecule diagram of $Rb^+(15C5)_2$ in I.

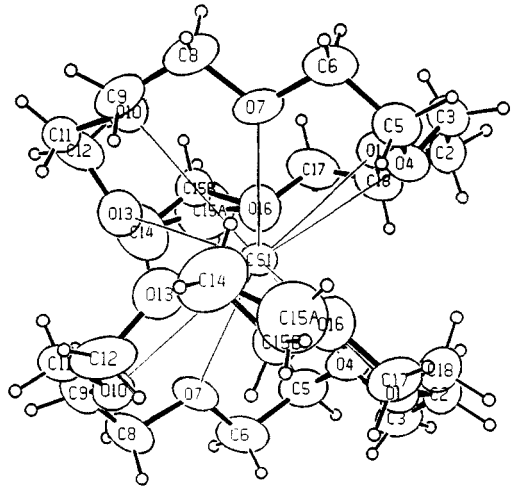

Figure 2. Single molecule diagram of $Cs^+(18C6)_2$ in II.

Results

The pertinent crystallographic data are given in Table I and final positional parameters are listed in Tables II and III for $Rb^+(15C5)_2Na^-$ and $Cs^+(18C6)_2Na^-$, respectively.[43] Positional and thermal parameters for $Cs^+(18C6)_2e^-$ have been previously reported.[26] Table IV contains selected values of bond distances in the three compounds. The structures of the single molecules in I and II are shown in Figures 1 and 2, respectively.

All three structures share similar features: in all cases the ions are coordinated by the eight nearest counterions, and have six next nearest neighbor ions of like sign. The ionic packing is such that the structure is primarily determined by close packing of the complexed cation, with Na^- occupying the resulting vacancies in the sodides. The cation packing in $Cs^+(18C6)_2e^-$ is nearly identical with that in $Cs^+(18C6)_2Na^-$.

In the course of refining the structures of each of the two sodides, at least one atom in the unique crown ether ring had abnormally high temperature factors associated with it, C8 in $Rb^+(15C5)_2Na^-$ and C15 in $Cs^+(18C6)_2Na^-$. It was assumed that this indicated some disorder in the flexible ring, so two unique positions with half-occupancy were introduced with subsequent improvement in temperature factors, agreement factors, and overall shift to error ratios. More detailed descriptions of the structures of $Rb^+(15C5)_2Na^-$ and of the sodide and electride of $Cs^+(18C6)_2$ are given below, with particular emphasis on the local environments of the ions.

(43) The structures of the two sodides were described by: Ward, D. L.; Dawes, S. B.; Fussa, O.; and Dye, J. L. *Abstracts, American Crystallographic Association Proceedings, Series 2*, 1985; Vol. 13, p 25.

Table V. Distances (Å) between the Anions and Their Nearest Atoms[a]

$Rb^+(15C5)_2Na^-$	$Cs^+(18C6)_2Na^-$	$Cs^+(18C6)_2e^-$[c]
[4] 3.80 (H8ba)	[2] 3.54 (5) (H6b)	[2] 3.29 (H6a)
[4] 4.15 (7) (H3b)	[2] 3.73 (5) (H2a)	[2] 3.64 (H15b)
[4] 4.17 (H8bb)	[2] 3.93 (H15ab)	[2] 3.76 (H2a)
[4] 4.25 (8) (H5a)	[2] 3.97 (H15bb)	[4] 4.09 (H17a)
[4] 4.39 (7) (H2a)	[2] 4.15 (6) (H3b)	[2] 4.17 (H15a)
[4] 4.42 (2) (C8b)[b]	[2] 4.18 (H15ba)	[2] 4.19 (C6)[b]
	[2] 4.23 (5) (H17a)	[2] 4.24 (H3a)
	[2] 4.43 (4) (H5b)	[2] 4.29 (H8b)
	[2] 4.46 (5) (H8b)	
	[2] 4.49 (5) (C6)[b]	

[a] Key: [multiplicity] distance (atom). [b] Carbon atoms. [c] Distances from e^- are calculated from the inversion center at 0, $^1/_2$, 0.

$Rb^+(15C5)_2Na^-$. The unit cell is *C*-centered monoclinic with both Rb^+ and Na^- occupying special positions on the lattice. The Rb^+ ion, with fractional coordinates $^1/_2$, 0, $^1/_2$, lies on a $2/m$ inversion center. Each cation is complexed by two 15-crown-5 molecules (Figure 1). Only half of one of them is unique because of the symmetry of the cationic site. The sodium anion, with fractional coordinates $^1/_2$, $^1/_2$, 0, also lies on a $2/m$ inversion center. The ionic packing can be described with respect to planes parallel to the a–b plane. Such planes at $z = 0$ contain only anions at the cell corners and planar face centers that are 8.92 Å from four neighboring coplanar anions, and 9.96 Å from anions at $\pm c$. Planes parallel to a–b at $z = ^1/_2$ contain only cations that stack at the centers of the a–c and b–c cell faces. The cations maintain the same distances from like ions as do the anions and are separated from neighboring anions with distances as follows: 7.49 Å to two anions along a cation–anion vector parallel to (1, 0, −1) and 7.76 Å to two anions along a cation–anion vector parallel to (1, 0, 1). These interionic distances are given in Table IV.

The sandwiched Rb^+ has a nearest oxygen distance of 2.99 Å. The sum of the cationic radius and the van der Waals radius of oxygen is only 2.88 Å, which indicates that the two crown ethers are limited in their approach to the cation by steric interference with each other.

The Na^- anion occupies a cavity between eight complexed cations, whose $-CH_2-$ protons are directed toward the anion, so as to form slightly anisotropic hydrogenic surroundings. The distances to the nearest protons from Na^- are listed in Table V. The shortest distance, 3.80 Å, implies a minimum sodium anion radius of 2.60 Å, assuming a hydrogen radius of 1.20 Å. The average van der Waals contact distance to the 20 nearest protons is 2.91 Å.

$Cs^+(18C6)_2Na^-$. The final positional parameters for $Cs^+(18C6)_2Na^-$ are given in Table III. Initial refinements resulted in unusually large thermal displacement parameters for C15, presumably because of disorder in the crown ether. Significant improvement of both the agreement factors and the thermal parameters of C15 was obtained by introducing two positions for C15 separated by 0.5 Å, each with fixed half-occupancy, and by constraining the hydrogens on C14 and both C15's to ride on the carbon atoms with fixed bond lengths and thermal parameters.

A molecular diagram of $Cs^+(18C6)_2Na^-$ is shown in Figure 2. The ionic packing in this compound is similar to the packing in $Rb^+(15C5)_2Na^-$. The anions in the cesium salt lie in planes at $z = 0$, $^1/_2$, etc. and form stacks in the z direction at the midpoints of the cell edges. The cations in the $C2/c$ space group lie on a 2-fold rotation axes parallel to b and have coordinates 0, b, $^1/_4$; 0, $-b$, $^3/_4$; etc. for the corners and center positions of an a–b plane at $z = ^1/_4$, $^3/_4$, etc. The face-centered plane of cations is displaced from $b = 0$, $^1/_2$, etc. by +0.328 Å at $z = ^1/_4$ and by −0.328 Å at $z = ^3/_4$. This displacement is the most significant difference in packing from that of $Rb^+(15C5)_2Na^-$. It requires that the unit cell dimension be doubled in the c direction. Interionic distances are listed in Table IV and are somewhat larger in $Cs^+(18C6)_2Na^-$, reflecting the increased size of the complexed cation. Each sodide ion has eight neighboring cations, two at each of four distances ranging from 7.9 Å to 9.3 Å. There is a strong

anisotropy in the nearest distances between like ions. The two adjacent anions along the *c* direction are 8.71 Å from the central anion while the four like anions in the *x*–*y* plane are separated by 10.37 Å.

The complexed cation consists of one unique crown ether; the second complexant is generated by a 2-fold rotation about an axis parallel to the *b* axis at the Cs^+ position. The mean plane of the oxygens in the crown ether is parallel to the *b* axis and makes a 25° angle with the *c* axis when projected onto the *a*–*c* plane. The orientations of the crown ether sandwiched cations are such that the hole of a given crown ether is filled by electron density from carbons and hydrogens of the nearest crown ether associated with an adjacent cation along the *c* direction. The average Cs–O distance is 3.357 Å; significantly longer than the mean Cs–O distance (3.15 Å) observed in 1:1 complexes of 18C6 with Cs^+.[44] Indeed, the sum of the ionic radius of Cs^+ and the van der Waals radius of oxygen is 3.2 Å. The long distance for the Cs–O interaction in $Cs^+(18C6)_2Na^-$ indicates that the cationic size is not the limiting factor in determining how closely the two crown ethers may approach each other; the two crown ethers make van der Waals contact with each other before they are fully in contact with the cation. As a result, the Cs^+ ion in a sandwich 18C6 complex is extremely well shielded from external influences.

The Na^- ion occupies an inversion center in the lattice, and is again bounded primarily by the hydrocarbon backbone of the crown ether molecule. The nearest contacts to Na^- are included in Table V. The closest contact distance to Na^- is 3.54 Å to two hydrogens, which implies a minimum ionic radius of 2.34 Å. The anionic cavity formed by the 18 nearest hydrogens to the anion yields an "effective" radius of 2.87 Å.

$Cs^+(18C6)_2e^-$. The structural details for $Cs^+(18C6)_2e^-$ have been previously reported.[26] For completeness, selected interionic distances as well as bond distances are included in Table IV. The structure of the electride is nearly identical with that of the sodide. The major differences in the packing of the lattice are (1) slightly different unit cell parameters and (2) a slightly larger distortion of Cs^+ positions from the corners and center of the unit cell in planes at $z = {}^1/_4, {}^3/_4$, etc. The conformation of the crown ether and the distances and angles all fall close to the values seen in the sodide.

A remarkable aspect of the structure of $Cs^+(18C6)_2e^-$ is that while the anion cavity has similar dimensions to the Na^- cavity, the electron density in the cavity is below the noise level on the final difference Fourier map. The noise level was 0.07 e/Å^3. The cavity is located at an inversion center in the lattice.

If it is assumed that the hydrogens lining the anionic cavity maintain a van der Waals radius of 1.2 Å, then an effective radius of the cavity may be estimated. The closest hydrogens are 3.29 Å from the inversion center, which implies a minimum cavity radius of 2.09 Å. The nearest 10 hydrogens yield a mean radius of 2.59 Å. As described later, however, the cavity shape is substantially nonspherical.

Discussion

Anionic Radius of Na^- from Crystal Structures. The minimum "hard-sphere" radius of the sodium anion in the two salts, as determined from contact with neighboring protons, is 2.60 Å for the rubidium salt and 2.35 Å for the cesium salt. The Na^- radius obtained by a similar analysis for the sodide $Na^+(C222)Na^-$ is 2.2 Å.[2] It is likely that Na^- is easily deformed so that some hydrogens may penetrate into the 3s electron density. We estimate that the "effective" radius of Na^- is 0.4–0.5 Å larger than the minimum radius.

Nature of the Electron Cavity in $Cs^+(18C6)_2e^-$. The presence of trapped electrons as anionic constituents in condensed-phase materials is well-known, most prominently as solvated electrons in alkali-metal solutions in ammonia, and as *F*-center defects in alkali-metal halide salts. The effective radius of the solvated electron in metal–ammonia solutions was estimated from measurements of the excess volume of solution of metals to be ~3 Å.[34] Copeland, Kestner, and Jortner have modeled the solvated electron in metal–ammonia solutions by a semicontinuum calculation[35] in which the cavity radius is an adjustable parameter. Energy minimization occurred when the cavity radius was 2.0 ± 0.3 Å. Kevan et al.[36,37] have also used a semicontinuum approach to estimate the radius of the electron trap in water and alcohols to range from 2 to 3 Å. Electron spin-echo modulation analysis of hyperfine coupling of protons to electrons trapped in glasses of NaOH, water and alcohols yielded cavity radii consistent with those obtained theoretically.[38] In all cases the electron density is presumed to penetrate beyond the boundaries of the trapping site. It should be noted, however, that cavity-free models of the solvated electron have also been proposed.[39,40]

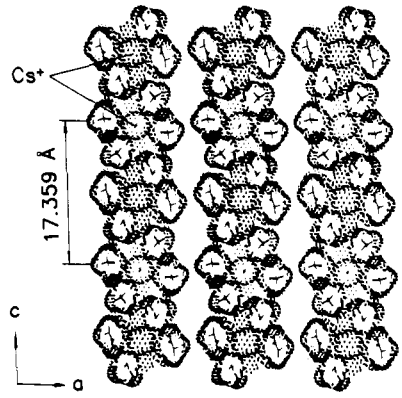

Figure 3. Cross-sectional view down the *b* axis in $Cs^+(18C6)_2e^-$ showing the "football-shaped" channels along the *c* axis.

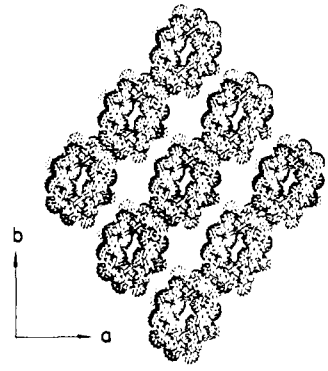

Figure 4. Cross-sectional view of a cavity down the *c* axis of $Cs^+(18C6)_2e^-$ showing the shape of the *c* channels at the maximum cross section and the channels that connect the cavities in the *a*–*b* plane. Similar channels at right angles are hidden in this view by projections of the crown ether molecules.

The anion vacancy in $Cs^+(18C6)_2e^-$, which has nearly the same shape and size as the anionic site in $Cs^+(18C6)_2Na^-$, appears to share many of the characteristics of the solvated electron cavity, but in contrast to the behavior in liquids, the cavity is relatively rigid, fixed by lattice packing constraints. The minimum radius of the cavity is 2.2 Å, well within the range discussed for cavities in solution. Yet there is no evidence of strong e^-–e^- interaction in the magnetic susceptibility, although electron exchange is fast on the ESR time scale.[18]

To better understand the nature of the electron cavities and the packing of the complexed cations around them, packing diagrams of the van der Waals surfaces were generated from the crystal structure on an Evans and Sutherland PS 300 graphics computer. Although these views refer to the electride structure, the corresponding views for the sodide are virtually indistinguishable. Several views of the packing around a cavity are shown in Figures 3–5. The cavity is completely enclosed by the eight nearest complexed cations, with only small channels of void space that connect each cavity with the six nearest anionic cavities. Figure 3 shows a stack of cavities along the *c* direction as viewed down the *b* axis. The cavities are elongated with a nearly square

(44) Dunitz, J. D.; Dobler, M.; Seiler, P.; Phizackerley, R. P. *Acta Crystallogr.* **1974**, *B30*, 2733.

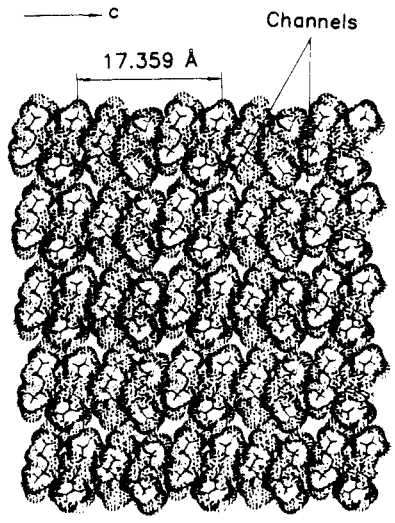

Figure 5. Cross-sectional view down the (1, 1, 0) direction of $Cs^+(18C6)_2e^-$. The open spaces are the small channels in the *a–b* plane that connect the cavities.

cross section ~5 Å on a side midway between the planes of complexed cesium cations. A short channel of minimum diameter ~2 Å connects the cavities along the *c* axis. Figure 4 is a cutaway view along the *c* axis at the midpoint of the cavities. The channels that lead to adjacent cavities in the same *a–b* plane occur along vectors [1, 1, 0] and [1, −1, 0] at the position of the greatest cross-sectional area. These channels are both smaller in cross section and longer through the constricted region of the channel than those along the *c* axis. Adjacent cavities in these directions are 10.2 Å apart. Any electron–electron interaction in this material might be expected to be anisotropic, favoring stronger interactions between adjacent electrons along the *c* axis, both because cavities in the *c* direction are closer together than those in the *a–b* plane and because the connecting channels are less constricted. Before the effect of channel dimensions can be assessed, however, we need to know more about the electronic penetration into the region occupied by the crown ethers. Figure 5 shows a view of a stack of complexed $Cs^+(18C6)_2$ cations down a [1, 1, 0] vector with the *c* direction horizontal. The constrictions of the channels leading to cavities are apparent as small void spaces. Note the efficiency with which the sandwiched cations are able to nearly fill space.

The optical spectrum, conductivity, and magnetic susceptibility of $Cs^+(18C6)_2e^-$ indicate that the electron is localized at sites that preclude any strong electron–electron interaction or electron–cation interaction. A reasonable picture of electron trapping in $Cs^+(18C6)_2e^-$ is that each electronic wave function is centered at an anionic site (cavity) with weak overlap between adjacent electrons and between the electron and Cs^+ and with an unknown amount of overlap with the $-CH_2-$ groups that line the cavity.

Structural Information from Solid-State NMR Studies. Solid-state NMR studies of salts that contain either or both of the nuclei ^{23}Na or ^{133}Cs are informative because both are highly sensitive nuclei with reasonable quadrupole coupling constants. The sources of line broadening for static lines in addition to that due to quadrupolar interactions are dipolar coupling to neighboring magnetic nuclei and anisotropic chemical shifts. In the case of a spherical anion such as Na^- with nuclear spin $I = {}^3/_2$, only dipolar coupling with hydrogen nuclei of spin $S = {}^1/_2$ contributes significantly to the static line width. The static line width of Na^- in $Na^+(C222)Na^-$ due to dipolar coupling to all hydrogen atoms within a distance of 7.0 Å was calculated with the Van Vleck equation[41] to be 2860 Hz. The observed line width is 2800 Hz.[25] Dipolar line widths of 1350 and 2520 Hz were calculated for the cesium cation and the sodide anion respectively by using the hydrogen to ion distances obtained at 213 K from the crystal structure of $Cs^+(18C6)_2Na^-$, including all hydrogens within 7.0 Å. Observed line widths were 1200 Hz for Cs^+ and 2300 Hz for Na^- at temperatures below 230 K. Above this temperature the lines narrowed, reaching 900 and 1300 Hz, respectively. This narrowing suggests the onset of rapid motion of the hydrogens relative to the nuclei of cesium and sodium, which partially averages the dipolar field at the ionic nuclei. For this narrowing to result from a phase change alone would require unrealistic increases in hydrogen-to-ion distances. Apparently, the dynamic disorder in the crown ether molecules, already apparent for one $-CH_2-$ group at 213 K, increases with increasing temperature.

Perhaps the strongest evidence for electron localization at the anionic sites in $Cs^+(18C6)_2e^-$ is the ^{133}Cs NMR pattern obtained in the mixed electride–sodide system.[30] The appearance of three peaks in addition to those of the pure electride and the pure sodide and the chemical shifts of these peaks clearly show that one, two, or three Na^- ions may substitute for e^- around a given complexed cesium cation. Since the electride and the sodide are isostructural, it is reasonable to assume that when crystals are grown from a solution that contains both Na^- and e^-_{solv}, a given anionic site may contain either Na^- or e^-. Since Na^- is diamagnetic, the substitution of it for a localized electron reduces the paramagnetic shift of Cs^+. Attempts to force more than three sodide ions into sites around the Cs^+ ion resulted in phase separation. The presence of only one peak for Cs^+ in the separate $Cs^+(18C6)_2Na^-$ phase shows that it is not possible to replace Na^- in the pure sodide by substantial concentrations of localized electrons although small concentrations are readily detected by ESR spectroscopy.[18]

In conclusion, the NMR evidence and the electrical, magnetic, and optical properties of $Cs^+(18C6)_2e^-$ and the similarity of the structure to that of $Cs^+(18C6)_2Na^-$ strongly favor a "stoichiometric *F*-center" model of the electride in which the electrons are trapped at anionic sites and interact only weakly with one another and with the complexed cation. In contrast to a "normal" anion, however, we anticipate that the electronic wave function does not go to zero at the boundary of the anionic site, but rather penetrates into the surrounding region. Thus, while electrides contain the lightest anion, the electron, it is unlikely that it is the simplest anion.

Acknowledgment. This research was supported in part by National Science Foundation Solid State Chemistry Grants DMR 84-14154 and DMR 87-14751. The X-ray diffractometer system was funded in part by NSF Chemical Instrumentation Grant CHE 84-03823. We are grateful to the Michigan State University Center for Fundamental Materials Research for providing some of the instrumentation used in this work. We thank Dr. Mark Kuchenmeister for assistance with the graphic displays of structures.

Supplementary Material Available: Table SI, listing crystal data and experimental details of the structure determination of I and II, tables listing positional parameters, general temperature factor expressions (*U*'s), bond distances, bond angles, and least-squares planes for I and II, and stereoviews of the unit cells of I and II (19 pages); tables of calculated and observed structure factors for I and II (41 pages). Ordering information is given on any current masthead page.